Bioorganic Chemistry 138 (2023) 106624

Contents lists available at ScienceDirect

Bioorganic Chemistry

journal homepage: www.elsevier.com/locate/bioorg

Next generation of selenocyanate and diselenides with upgraded leishmanicidal activity

Andreina Henriquez-Figuereo [a,b], Mercedes Alcon [d], Esther Moreno [a,b,c,*], Carmen Sanmartín [a,b,c,*], Socorro Espuelas [a,b,c], Héctor de Lucio [d], Antonio Jiménez-Ruiz [d], Daniel Plano [a,b,c]

[a] University of Navarra, Faculty of Pharmacy and Nutrition, Department of Pharmaceutical Technology and Chemistry, Pamplona, Spain
[b] Institute of Tropical Health, University of Navarra, ISTUN, Pamplona, Spain
[c] IdisNA, Navarra Institute for Health Research, Pamplona, Spain
[d] Universidad de Alcalá, Departamento de Biología de Sistemas, 28805 Alcalá de Henares, Madrid, Spain

ARTICLE INFO

Keywords:
Selenocyanate
Diselenide
Leishmanicidal agents
Selenocompounds
Trypanothione reductase

ABSTRACT

Nowadays, leishmaniasis is still treated with outdated drugs that present several obstacles related to their high toxicity, long duration, parenteral administration, high costs and drug resistance. Therefore, there is an urgent demand for safer and more effective novel drugs. Previous studies indicated that selenium compounds are promising derivatives for innovative therapy in leishmaniasis treatment. With this background, a new library of 20 selenocyanate and diselenide derivatives were designed based on structural features present in the leishmanicidal drug miltefosine. Compounds were initially screened against promastigotes of *L. major* and *L. infantum* and their cytotoxicity was evaluated in THP-1 cells. Compounds **B8** and **B9** were the most potent and less cytotoxic and were further screened for the intracellular back transformation assay. The results obtained revealed that **B8** and **B9** showed EC_{50} values of 7.7 μM and 5.7 μM, respectively, in *L. major* amastigotes, while they presented values of 6.0 μM and 7.4 μM, respectively, against *L. infantum* amastigotes. Furthermore, they exerted high selectivity ($60 < SI > 70$) towards bone marrow-derived macrophages. Finally, these compounds exhibited higher TryR inhibitory activity than mepacrine (IC_{50} 7.6 and 9.2 μM, respectively), and induced nitric oxide (NO) and reactive oxygen species (ROS) production in macrophages. These results suggest that the compounds **B8** and **B9** could not only exert a direct leishmanicidal activity against the parasite but also present an indirect action by activating the microbicidal arsenal of the macrophage. Overall, these new generation of diselenides could constitute promising leishmanicidal drug candidates for further studies.

1. Introduction

Leishmaniasis encompasses a group of parasitic protozoan diseases transmitted to humans through the bite of female sandflies belonging the genera *Phlebotomus* and *Lutzomyia* [1]. Currently, leishmaniasis is still considered a neglected disease due to low interest and lack of funding for developping novel effective treatments [2–4]. Leishmaniasis affects 12 million people and 350,000 are at risk of infection according to the World Health Organization (WHO) [5]. During their life cycle, parasites present two main stages: promastigote (in the vector) and amastigote (in the host) [6]. Once the number of parasites inside macrophages increases, cells will be lysed and amastigotes will be released into the surrounding tissues where they will be phagocytosed by other uninfected macrophages, spreading the infection. The infected macrophages will produce toxic mediators such as reactive oxygen species (ROS) and nitric oxide (NO), which constitute important weapons in the control of the infection [7]. To avoid destruction and evade the host immune response, parasites alter certain macrophage defence functions, such as oxidative damage, ability to present antigens, and apoptosis. There are three main clinical manifestations of leishmaniasis, depending on the strain of the parasite and the immune status of the host: i) cutaneous leishmaniasis [8] (the most common type) causing skin lesions at the site of the sandfly bite, ii) visceral leishmaniasis [9] (the most severe form of the disease) also known as kala-azar, which manifests with hepatomegaly, splenomegaly, anaemia, and weight loss which finally lead to the death of the patient if untrated, and finally iii)

* Corresponding authors at: Department of Pharmaceutical Technology and Chemistry, University of Navarra, 31008 Pamplona, Spain.
E-mail addresses: emorenoa@unav.es (E. Moreno), sanmartin@unav.es (C. Sanmartín).

https://doi.org/10.1016/j.bioorg.2023.106624
Received 28 March 2023; Received in revised form 8 May 2023; Accepted 21 May 2023
Available online 24 May 2023

mucocutaneous leishmaniasis [10] whose main effect is the destruction of the mucous membranes of the mouth, nose and throat [10]. Despite the existence of drugs for the treatment of the disease, they are ineffective in controling the infection and preventing its progression. Moreover, current treatment protocols are problematic due to their high toxicity and long-time administration, which complicate the patient adherence to treatment. Some of the drugs include pentavalent antimonials, amphotericin B [11] (AmB), miltefosine [12] (MIL) and paromomycin [13] (PMN), which currently constitute the therapeutic protocol against this disease. However, their high costs and therapeutic complications have limited their use [5]. In addition, the emergence of resistant strains [14] and the existence of several parasite survival pathways makes the development of new drugs an urgent need [14]. This situation is aggravated by the disinterest of pharmaceutical companies in developing new leishmanicidal drugs, mainly because many parasitic diseases are present in countries with few economic resources that can barely afford the high costs [4].

Selenium (Se) is considered a vital element and deeply involved in the defence mechanisms of the human immune system [15]. Se levels are related to innate and adaptive immune responses to bacterial and parasitic infections [16,17] and adequate supplementation can help the immune system [18] to eliminate these pathogens, through the antioxidant properties of some selenoproteins [19,20]. Depending on the chemical form, the mechanism of action of Se presents different pathways [21]. On the other hand, the inclusion of different Se functionalities (methylselenol, selenocyanate and diselenide) into organic molecules offers an innovative design strategy in the search for new bioactive compounds against parasitic diseases such as leishmaniasis. In recents years, our group has used rational design to obtain a new generation of selenocyanate and diselenide derivatives with potent and selective anti-leishmanial activity both *in vitro* and *in vivo* [22–24]. Moreover, some of them were trypanothione reductase (TryR) inhibitors [1,23–27].

Currently available literature has pointed out great attention on MIL for its oral clinical applications in leishmaniasis treatment. Given that one of the chemical features of MIL is the presence of alkyl chains, in the present study we have mainly focused on structural modifications using diversification of aliphatic carbon chain length from 3 to 15 carbon atoms. On the topic of optimal chain substitution, we were also interested in analyzing the impact of the inclusion of carbocycles with different ring size (3–6 members) in the biological activity.

In this context, and motivated by the positive outcome of previous studies [27,28], we embarked on this follow-up research to assess the impact of of the aliphatic decarion mentioned above on the parent selenocyanate (**A0**) and diselenide (**B0**) derivatives over their leishmanicidal activity. The set of the 20 new compounds were designed and synthesized (Fig. 1) taking into account the commercially available acid chlorides.

The leishmanicidal activity of the compounds (**A1-10** and **B1-10**) were evaluated against promastigotes and amastigotes of *L. major* and *L. infantum* and their cytotoxicity was tested against THP-1 cells. Furthermore, in order to investigate the therapeutic potential of the synthesized compounds, drug combination studies with the drugs MIL, PMN and AmB were carried out. Finally, to elucidate the mechanism of action of the lead molecules, trypanothione reductase (TryR) inhibition as well as ROS and NO production assays were also performed.

2. Results and discussion

2.1. Chemistry

Our research group has developed potent leishmanicidal Se derivatives, including selenocyanates and diselenides [25,26,28]. A library of lipophilic derivatives containing Se in the form of selenocyanate or diselenide were grouped in series **A1-10** and **B1-10**, respectively. The synthesis of the compounds was carried out following the synthethic route depicted in Fig. 2 as previously described [24,28]. Selenocyanate derivatives **A1-10** were obtained from the intermediate 4-aminophenyl selenocyanate (**A0**) by reaction with different acid chlorides. The ease of purification by washing with *n*-hexane and the good yields obtained for most of the compounds in this series (>40%) placed them in an advantageous position in the development of new leishmanicidal agents. Furthermore, the synthesis of their diselenide counterparts (**B1-4** and **B7-10**) was carried out by reduction of the corresponding selenocyanates with sodium borohydride in ethanol. The diselenides were obtained in yields ranging from 24 to 67%. Unfortunately, compounds **B4**, **B5** and **B6** could not be obtained by this method and an alternative synthetic route was carried out. For this purpose, the intermediate bis(4-aminophenyl)diselenide (**B0**) was synthesised from the reduction with sodium borohydride of intermediate **A0**, which was reacted with the corresponding acid chlorides in a molar ratio of 1:2 in acetone and potassium carbonate for 2 h, yielding a yellow solid. By using this alternative synthetic route, it was possible to isolate yellow solids, corresponding to derivatives **B4, B5** and **B6.** As mentioned above, one of the main obstacles in the treatment of leishmaniasis is the cost of treatment as well as the complications of the drug development process. To overcome these obstacles, the synthetic process followed in the course of this research showed versatility, simplicity and economic profitability due to the low cost of the reagents and solvents used, which would favour the development of new therapeutic and low cost alternatives for parasitic diseases such as leishmaniasis.

All the compounds obtained during this research were stable at room temperature (r.t.). The determination of the purity of the final compounds and the intermediates was carried out by thin layer chromatography (TLC) and nuclear magnetic resonance (NMR). The ^{1}H-, ^{13}C- and ^{77}Se- NMR spectra can be found in the Supplementary Material

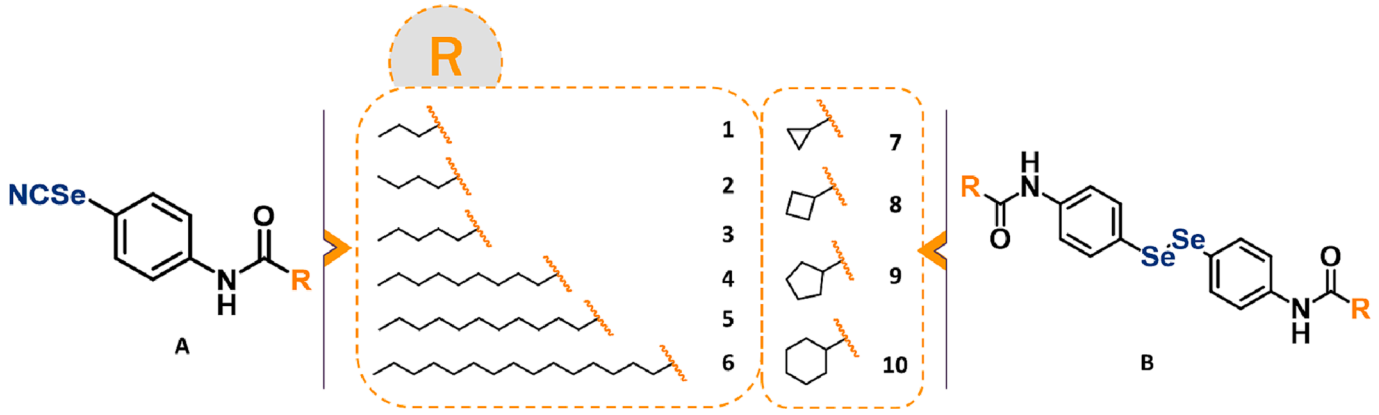

Fig. 1. General structure for the 20 selenocyanate (**Serie A**) and diselenide (**Serie B**) derivatives synthetized in this study.

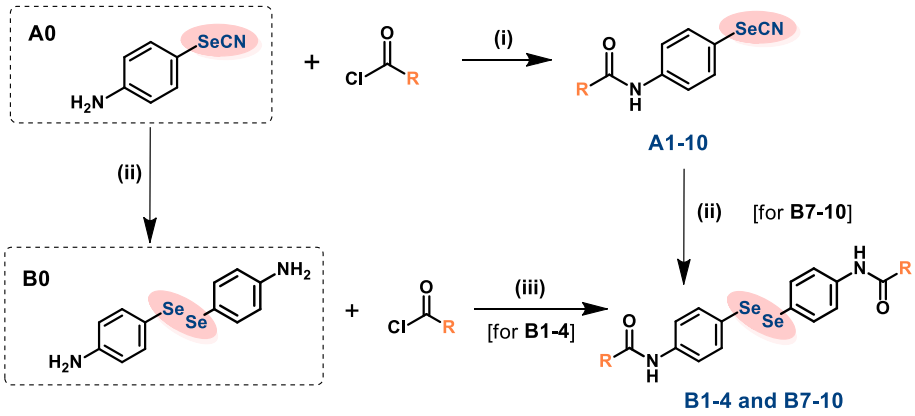

Fig. 2. Synthetic route of the reported seleno compounds (A1-10 and B1-10). The reagents and conditions used were as follows: (i) DCM, K_2CO_3, r.t., 24 h; (ii) $NaBH_4$, EtOH, r.t., 2–24 h; (iii) DCM, TEA, r.t., 24 h.

(Figures S3-S56).

2.2. Leishmanicidal activity against Leishmania promastigotes and cytotoxicity in THP-1 cells

Selenocyanate and diselenide derivatives (**A1-10** and **B1-10**) were initially tested against promastigotes of *L. infantum* and *L. major* according to a previously described procedure [27]. Derivatives **B5** and **B6**, despite being isolated, could not be characterized and biologically evaluated due to solubility problems. Most of the compounds showed remarkable leishmanicidal effect against both strains (Table 1). Derivatives **A1-A5**, **A8-A10**, **B1**, and **B7-B9** were more active than the reference drugs with EC_{50} below 10 μM after 48 h of treatment. Current treatment drugs have several drawbacks, including toxicity. For that reason, the citotoxicity of the compounds was screened against the human monocytic leukaemia cell line THP-1 [29]. Results showed that diselenide derivatives were less toxic than selenocyanates. Derivatives **B8** and **B9**, containing cyclobutane and cyclopentane respectively, presented remarkable bioactivity and selectivity. Compared with the structurally related first generation of diselenides published by our research group (compounds bis(4-aminophenyl)diselenide [28], 2,2'-[(diselenodiyldibenzene-4,1-diyl)dicarbamoyl]bis(cyclohexanecarboxylic acid) and 3,3'-[(diselenodiyldibenzene-4,1-diyl) dicarbamoyl]bis(7- oxabicyclo[2.2.1]hept-5-ene-2-carboxylic acid) [25]), both derivatives show comparable leishmanicidal activity against promastigotes (EC_{50} values of 7.7 μM for **B8**, 6.5 μM for **B9**, and 11.2 μM for compound 2a) and amastigotes (EC_{50} values of 1.2 μM for **B8**, 1.1 μM for **B9**, 10.6 μM for C.I.7, and 1.3 μM for C.I.8) of *L. infantum*. Otherwise, compounds **B8** and **B9** present greater selectivity than previously reported lead compounds (selectivity indexes of 54 for **B8**, 66 for **B9**, 24 for 2a, >12 for C.I.7, and > 19 for C.I.8). Indeed, the presence of a lipophilic tail could give these compounds improved leishmanicidal activity, as they might be more permeable to cell membranes. This fact, together with the presence of the diselenide group, which has shown potent activity against several strains of *Leishmania,* both *in vitro* [25] and *in vivo* [23], may explain the activity exhibited by compounds **B8** and **B9**. Compound **B9** was the most selective one, even more than PMN in *L. major* (196-fold) and *L. infantum* (110-fold) promastigotes. Different authors have affirmed that leishmanicidal candidates must exert SI values > 20 [30–33]. The results obtained allowed us to consider compounds **B8** and **B9** as lead compounds for further evaluation.

Table 1
EC_{50} values of the synthetized compounds against promastigotes of *L. major* and *L. infantum* and cytotoxic activity against THP-1 cells after 48 h of treatment.

	Promastigotes *L. major*	Promastigotes *L. infantum*	THP-1 cells	[c]SI	
Ref.	[a]EC_{50} (μM)	[b]EC_{50} (μM)	CC_{50} (μM)	Promastigotes *L. major*	Promastigotes *L. infantum*
A1	7.1 ± 1.8	6.1 ± 1.7	6.4 ± 0.4	0.5	1.1
A2	5.2 ± 0.6	6.8 ± 1.8	1.2 ± 0.7	0.7	0.6
A3	2.6 ± 0.7	7.7 ± 1.7	3.1 ± 3.9	1.2	0.5
A4	1.1 ± 0.5	2.4 ± 0.1	2.2 ± 3.2	1.1	0.8
A5	5.9 ± 1.4	2.3 ± 0.1	0.3 ± 0.1	0.1	0.2
A6	54.5 ± 24.3	55.9 ± 32.4	0.6 ± 0.1	0.1	0.1
A7	12.9 ± 4.4	9.1 ± 2.7	56.1 ± 1.8	4.3	6.2
A8	4.4 ± 1.3	5.8 ± 2.8	52.2 ± 3.3	13.0	9.0
A9	7.7 ± 0.7	4.0 ± 1.9	47.7 ± 29.1	6.2	12.0
A10	9.5 ± 0.1	4.5 ± 0.9	66.8 ± 18.3	7.1	15.0
B1	8.7 ± 1.2	6.2 ± 2.3	216.1 ± 10.7	25.0	35.1
B2	14.6 ± 3.7	6.3 ± 0.1	473.0 ± 10.8	32.4	75.6
B3	429.5 ± 86.7	318.6 ± 175.1	141.4 ± 5.0	0.9	0.4
B4	693.9 ± 171.3	816.7 ± 18.3	255.6 ± 25.9	0.6	0.3
B7	8.0 ± 0.1	6.7 ± 1.4	127.9 ± 31.0	16.0	19.2
B8	6.1 ± 1.0	7.7 ± 1.1	414.1 ± 14.4	67.6	53.6
B9	3.7 ± 2.0	6.5 ± 0.2	430.9 ± 67.6	118.1	66.1
B10	23.2 ± 3.9	8.2 ± 0.1	465.8 ± 3.5	20.1	56.7
MIL	66.6 ± 1.1	31.9 ± 2.3	13.3 ± 2.8	0.2	0.4
PMN	71.0 ± 3.3	18.0 ± 1.0	39.0 ± 13.7	0.6	2.2

[a] Effective concentration (EC_{50}) is defined as the concentration that caused a 50% reduction of *Leishmania* promastigotes proliferation.
[b] Cytotoxic concentration (CC_{50}) is defined as the concentration required to obtain 50% of cell death.
[c] Selectivity index (SI) is the ratio of the CC_{50} against THP-1 cells and the EC_{50} in *Leishmania* promastigotes. N.D.: no data due to solubility problems. Results are expressed as mean ± SD of at least three independent experiments in triplicate.

2.3. Drug combination studies

The toxicity and side effects described by the use of the current therapeutic options for the treatment of leishmaniasis limit their efficacy [34]. To mitigate these complications, multiple cost-effective strategies have been used, such as drug combination [35]. Combination therapies present several advantages like reduction of treatment dose/regimen and delay of resistance emergence. The lead compounds (**B8** and **B9**) were assayed to determine their *in vitro* effect in *L. major* and *L. infantum* promastigotes when combined with the reference drugs MIL, PMN and AmB. For this purpose, fractional inhibitory concentration indexes (FICI) were calculated [36,37]. A fixed- ratio method for evaluating the nature of drug interactions was originally developed for antibacterial drugs and some modifications were successfully applied for antiplasmodial drugs [38]. In both species, **B8** (Table S1 and Figure S1 in the Supplementary Material) demonstrated no interaction with these drugs ($0.5 < FICI < 4$) while the effect of combination of compound **B9** and PMN proved to be antagonistic, showing a $FICI > 4$ (Table S1 and Figure S2 in the Supplementary Material). However, if we focused in the combination of MIL with the lead compounds, results showed that the EC_{50} of **B8** in *L. infantum* promastigotes reduced from 7.7 to 7.6–6.0 μM when different fixed-ratio solutions of MIL were added and, in the case of **B9**, its EC_{50} decreased from 6.7 to 4.8–4.2 μM. Besides, when different fixed-ration of MIL was mixed with **B8** and **B9** against *L. major* promastigotes, their EC_{50} were reduced from 6.1 to 6–4.9 μM and from 3.7 to 0.9–0.6 μM, respectively.

2.4. Leishmanicidal activity against Leishmania amastigotes and cytotoxicity in bone marrow-derived macrophages (BMDM)

For decades, axenic amastigotes have been used as a biological model for initial drug anti-*Leishmania* screening [39,40]. Therefore, the leishmanicidal activity of diselenides **B8** and **B9** was tested in this model. Results obtained against axenic amastigotes of *L. infantum* are gathered in Table 2. The lead compounds (**B8** and **B9**) showed potent leishmanicidal activity in this model, with EC_{50} values < 2 μM against axenic amastigotes of *L. infantum* after 24 h of treatment (1.1 and 1.2 μM, respectively). Compounds **B8** and **B9** (Table 2) were also evaluated by the BTA [41,42], a method that better mimicks the infection. This assay showed that these compounds exerted similar leishmanicidal activity on both *Leishmania* strains (EC_{50} below10 μM after 48 h of treatment). Finally, by Giemsa staining, EC_{50} values between 10 and 30 μM were found after 48 h of incubation with compounds, showing these diselenides higher activity in the *L. infantum* strain.

Results showed a dose-dependent reduction in the number of amastigotes per infected-macrophage in both strains for each compound. Compared to untreated infected cells, there was a significant decrease in the number of infected macrophages after treatment with the lead compounds (Fig. 3), being this reduction statistically significant at 10 and 20 μM. Compounds showed a similar reduction in the percentage of infection (arround 60%) at 20 μM in *L. infantum* infected-BMDM whereas this percentage was reduced to 50% in the case of *L. major*-infected macrophages. Surprisingly, these compounds were able to eradicate>50% of the amastigotes load at 20 μM with almost no toxic effects on BMDM. Compound derivatives **B8** and **B9** have shown remarkable leishmanicidal properties that may have positioned them as prominent therapeutic candidates, due to their low toxicity and promising leishmanicidal activity. A noteworthy feature of these compounds is the presence of the cyclobutane and cyclopentane substituents, which are a novel incorporation, allowing the derivatives to possess structural proximity and explaining the similarity in terms of leishmanicidal activity. The excellent activity of these compounds on axenic amastigotes corroborates how the incorporation of Se is a profitable strategy in the development of new molecules with leishmanicidal activity.

2.5. Mechanism of action of the lead compounds

Trypanothione reductase activity. To preliminaryly elucidate the mode of action of the diselenide derivatives **B8** and **B9**, we decided to evaluate their impact on the TryR enzyme. TryR is an enzyme that plays an important role in the regulation of redox balance and is exclusive of the parasite (it is not present in the mamalian host) [43]. These reasons make this enzyme an ideal target for new anti-*Leishmania* drugs. Mepacrine, a known TryR inhibitor, was used as a reference drug. Compounds **B8** and **B9** were found to posses higher inhibitory capacity against TryR than mepacrine *in vitro* (Table 3).

Some organoselenium compounds, such as ebselen and other isoselenazolones, have been found to exhibit irreversible inhibition of their targets [44]. Furthermore, the benzisothiazolone compound ebsulfur, a sulphur analogue of ebselen, is an irreversible inhibitor of *Trypanosoma brucei* TryR [45]. To investigate the irreversible nature of inhibition caused by our diselenides, we performed an incubation experiment in which TryR (400 nM) was treated with **B8** (25 μM) for 16 h, using the reversible inhibitor mepacrine (25 μM) as control. After incubation, enzyme and inhibitors were diluted 400 times at final concentrations of 1 nM and 62.5 nM, respectively, before starting the reaction. It is noteworthy that when enzyme and inhibitor are mixed directly at these concentrations, neither mepacrine nor **B8** noticeably reduce the reaction rate. The results, as depicted in Fig. 4A, reveal that the enzyme incubated with **B8** remains completely inactive throughout the entire assay period of 13 h, which demonstrates the irreversible nature of this inhibition. Analysis of the residual fractional activity of the enzyme at different inhibitor concentrations and pre-incubation times (Fig. 4B) allowed us to estimate the k_{obs} for the inactivation process at every inhibitor concentration. Representation of the different k_{obs} vs inhibitor concentration (Fig. 4C) allowed us to identify the rate constant for the inactivation ($k_{inact} = 0.14 \pm 0.03$ min^{-1}) and the $K_{i(irrev)}$ (90.1 ± 25.5 μM) for the process of irreversible inhibition [46]. It must be pointed out that similar to what happens to K_m, which is not the dissociation constant of the substrate, $K_{i(irrev)}$ is not the dissociation constant of the inhibitor but the concentration at which enzyme inactivation occurs a half the maximum velocity, which depends on the k_{on} and k_{off} values for the interaction between enzyme and inhibitor and also on the k_{inact}.

Despite the demonstrated capacity of **B8** to irreversibly inhibit TryR, the K_i value of 90.1 ± 25.5 μM obtained for this process does not fully explain the low IC_{50} value observed for this compound (7.6 μM), which

Table 2
Leishmanicidal activity of the lead compounds (**B8** and **B9**) against amastigotes and cytotoxicity in BMDM.

		Axenic amastigotes	*BTA assay*				*Giemsa staining*			
	BMDM	*L. infantum*	*L. major*		*L. infantum*		*L. major*		*L. infantum*	
Ref.	[a]CC_{50} (μM)	[b]EC_{50} (μM)	[b]EC_{50} (μM)	[c]SI	[b]EC_{50} (μM)	[c]SI	[b]EC_{50} (μM)	[c]SI	[b]EC_{50} (μM)	[c]SI
B8	462.2 ± 3.9	1.2 ± 0.1	7.7 ± 0.1	60	6.0 ± 0.8	76	27.7 ± 5.1	16.6	11.8 ± 5.6	39.1
B9	393.4 ± 11.3	1.1 ± 0.1	5.7 ± 1.3	68	7.4 ± 0.6	62	20.1 ± 3.2	19.5	17.7 ± 0.7	22.2

[a]Cytotoxic concentration (CC_{50}) is defined as the concentration required to obtain 50% of cell death.
[b]Effective concentration (EC_{50}) is defined as the concentration that caused a 50% reduction of *Leishmania* amastigotes proliferation. Selectivity index (SI) is the ratio of the CC_{50} against BMDM and the EC_{50} in *Leishmania* amastigotes. Results are expressed as mean ± SD of at least three independent experiments.

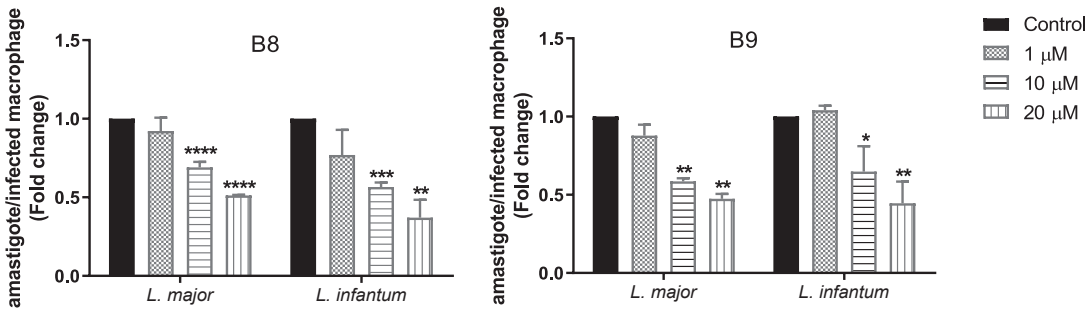

Fig. 3. Effect of selenocompounds **B8** and **B9** on *L. major* and *L. infatum* infected BMDM. Treatments with the compounds were performed at different concentrations (1, 10 and 20 μM) and graphs show the number of amastigotes per infected macrophage after 48 h of treatment. Controls represent untreated infected cells. Results indicate mean ± SD of three independent experiments. * $p < 0.0$, ** $p < 0.01$, *** $p < 0.001$ and **** $p < 0.0001$.

Table 3
In vitro IC_{50} values of the selected compounds (**B8** and **B9**) along with mepacrine (reference TryR inhibitor) towards TryR.

Ref.	TryR IC_{50} (μM)
B8	7.6 ± 0.9
B9	9.2 ± 0.9
Mepacrine	16.9 ± 1.2

[a]TryR, Trypanothione reductase. IC_{50}, 50% inhibitory concentration. Results are expressed as mean ± SEM (standard error of the mean).

suggest that there must be an additional mechanism of inhibition. To address this issue, the velocity of the reactions (V) was calculated at different concentrations of inhibitor and substrate (TS_2). The Lineweaver-Burk plot of $1/V$ vs $1/[TS_2]$ at different concentrations of **B8** is shown in Fig. 4D. The results are indicative of a competitive mode of inhibition against TS_2 and revealed a *Ki* value of 7.2 ± 1.4 μM. These results are now fully compatible with the IC_{50} value reported. Consequently, **B8** behaves as a competitive inhibitor that, in addition, is able to slowly inactivate the enzyme in the absence of a substrate.

Nitric oxide production in BMDM. NO is produced by the nitric oxide synthase [47] enzyme and it is critical to macrophage defence against pathogens such as *Leishmania* [7,48]. NO was measured in the supernatant of macrophages treated with compounds **B8** and **B9** for 48 h. The results obtained showed that both compounds activated macrophage to inciate the production of NO which could lead to the reduced infection observed. According to the obtained results (Fig. 5A), compounds **B8** and **B9** showed an increase in the NO production when drug concentration was augmented, showing a significant increase in NO production at 50 μM for both compounds and at 100 μM only for compound **B9** (~10-fold increase compared to untreated cells). In addition, these data suggest the possibility that these compounds are capable of modulating cell responses, leading to parasite death. A similar immunomodulatory effect is exhibited by miltefosine, which has been shown to increase NO production in macrophages [49].

ROS production assay. Multiple studies have shown the immunomodulatory effect of Se [50–53] and the Se levels influence the modulation of the immune response against infections caused by viruses and parasites [54]. Macrophage activity is also affected by Se levels [55]. *In vitro* assays have shown that Se supplementation improved phagocytosis, degranulation and ROS production after stimulation of macrophages [18]. ROS is generated by cells to fight against pathogenic infections [51]. This mechanism supports several anti-protozoal drugs used to combat intracellular parasites inside infected cells [52]. Treatment with **B8** and **B9** at different concentrations (20, 50 and 100 μM) induced ROS release in non-infected BMDM (Fig. 5B). ROS production could be observed after staining with H_2DCFDA, compared to the untreated control. Compounds **B8** and **B9** increased ROS generation by BMDM at 20 and 50 μM (increased by around 20%). However, only treatment of BMDM with compound **B9** at 100 μM resulted in a significant increment in their ROS production (*, $p < 0.05$, approximately 35% higher than the control). The anti-oxidant and pro-oxidant effects of the diselenide core confer attractive biological properties to these structures in the search for novel treatment drugs for parasitic diseases such as leishmaniasis [56].

2.6. Theorical ADME and Lipinski properties

Finally, the properties of absorption, distribution, metabolism and excretion (ADME) of the lead compounds were predicted (Table 4). Compounds were examined using the pkCSM software. Furthermore, Lipinski's rule of five values were analyzed. Lead compounds (**B8** and **B9**) only failed 1 of the Lipinski's 5 rules, the one related to the molecular weight. Human intestinal absorption effect (HIA) and Caco-2 permeability are considered valid indicators for drug absorption in the intestine. Predicted intestinal absorption values for compounds **B8** and **B9** were excellent.

3. Conclusion

In summary, a simple, one-step and cost-effective synthetic route for obtaining 20 new selenocyanates and diselenides has been achieved. The general structure of these derivatives is based on the structural features present in the reference drug MIL. The results obtained during the biological evaluation demonstrated that two diselenide derivatives (**B8** and **B9**) are excellent leishmanicidal agents on both promastigotes and amastigotes of *L. major* and *L. infantum*. The EC_{50} values obtained for both strains for compound **B8** (6.1 μM and 7.7 μM in promastigotes and 7.7 μM and 6.0 μM in amastigotes) and for **B9** (3.7 μM and 6.5 μM in promastigotes and 5.7 μM and 7.4 μM in amastigotes) are superior to the reference drugs MIL and PMN. Cytotoxicity evaluation of **B8** and **B9** derivatives on THP-1-derived macrophages showed low cytotoxicity and high selectivity (SI values of 67.6 and 53.6 for **B8** and 118.1 and 66.1 for **B9**), showing superior selectivity than the reference drugs. To elucidate the possible mechanism of action of these derivatives, their effects on TryR were evaluated. Both lead compounds showed a potent inhibitory effect on TryR (IC_{50} values of 7.6 μM and 9.2 μM for **B8** and **B9**, respectively), presenting lower IC_{50} values than mepacrine. Further studies on TryR showed that compound **B8** act as an irreversible competitive inhibitor (Ki value of 90.1 μM) in the absence of substrate. However, further studies would be necessary to evaluate other possible mechanisms of action involved in the leishmanicidal effect of this derivative. Finally, we can conclude that selenated derivatives constitute an upgraded starting point in the design of potent, safer and low-cost leishmanicidal agents.

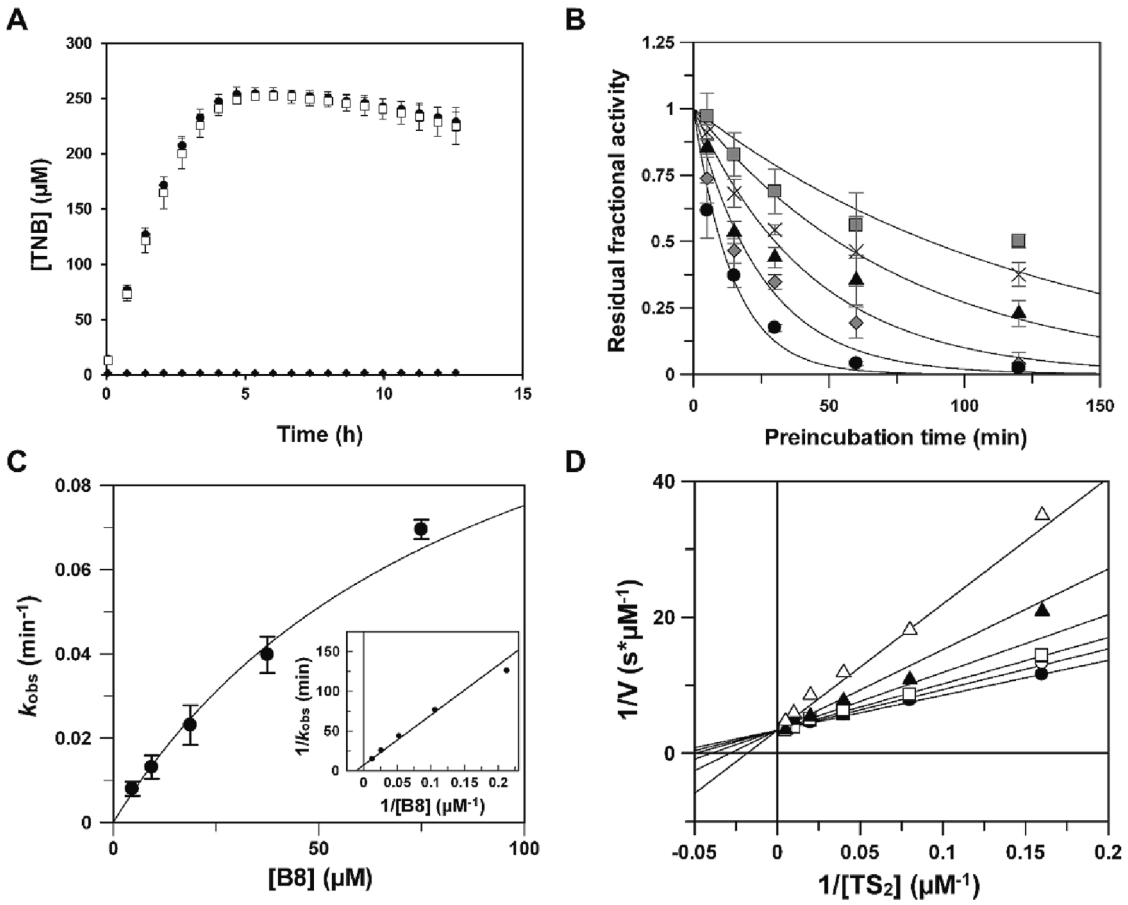

Fig. 4. Irreversible inhibition of TryR by **B8**. **(A)** TryR (400 nM) was preincubated during 16 h in the absence of inhibitor (●) or in the presence of 25 μM of mepacrine (□) or **B8** (♦). Samples were diluted (400 times) and TryR activity was evaluated in enzymatic reaction mixtures containing TryR (1 nM) in the absence of inhibitor or in the presence of 62.5 nM mepacrine or 62.5 nM **B8**. Production of 2-nitro-5-mercaptobenzoic acid (TNB) was monitored by increase in absorbance at 412 nm. The error bars indicate the standard deviations associated with each data point of three independent experiments. **(B)** Plot of residual activities of TryR. The enzyme (400 nM) was incubated during the indicated time periods in the presence of different **B8** concentrations: 4.69 μM (■), 9.38 μM (X), 18.75 μM (▲), 37.5 μM (◆) and 75 μM (●). Samples were diluted (400 times) and residual activity of TryR was evaluated. The residual activity is defined as the initial velocity (v_i) at each **B8** concentration relative to the initial velocity in the absence of inhibitor and without preincubation (v_0). Data were fitted to Equation (3) to obtain the k_{obs} values. The error bars indicate the standard deviations associated with each data point of three independent experiments. **(C)** Plot of the k_{obs} values for the curves shown in **(B)** as a function of **B8** concentration. Data were fitted to Equation (4) to obtain the $K_{i(irrev)}$ and k_{inact} values. The double-reciprocal plot is shown in the inset. The error bars indicate the standard error of the fits shown in **(B)**. **(D)** Lineweaver-Burk double-reciprocal plot of the initial velocity of the TryR oxidoreductase reaction as a function of TS_2 concentration measured at different **B8** concentrations: 0 μM (●), 1.17 μM (○), 2.34 μM (■), 4.69 μM (□), 9.38 μM (▲) and 18.75 μM (△). Data were fitted to Equation (2) to obtain the *K*i value. Results are representative of three independent experiments.

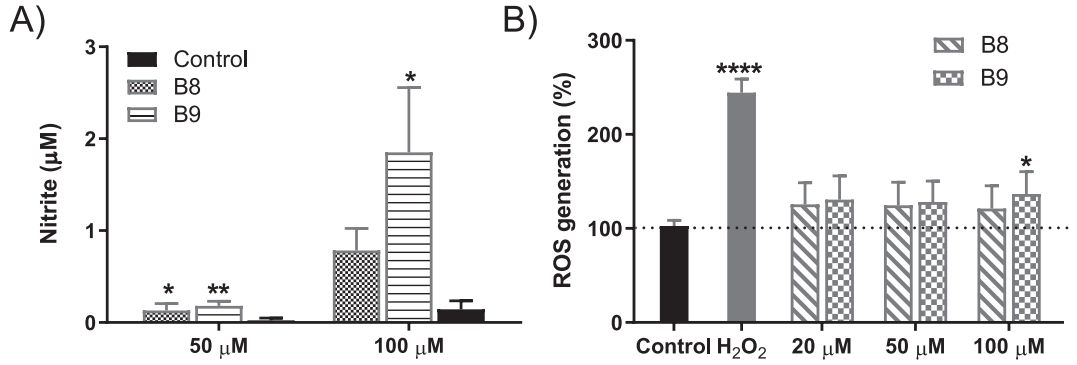

Fig. 5. (A) NO levels and (B) ROS produced by the lead compounds **B8** and **B9** in non-infected BMDM after 48 h of treatment. * $p < 0.05$, ** $p < 0.01$ and **** $p < 0.0001$.

Table 4
Theoretical insight into the absorption, distribution, metabolism, and excretion (ADME) properties and Lipinski violations for the lead compounds.

						Absorption		
Ref.	[a]*MW (g/mol)*	[b]*LogP*	[c] *OHNH-donors*	[d]*ON acceptors*	[e]*Lipinski violation*	[f]*GI absorption*	[g]*Water solubility*	[h]*Caco2*
B8	506.36	2.43	2	2	1	94.66	−3.65	0.97
B9	534.41	2.84	2	2	1	93.28	−3.68	0.98

[a] MW, molecular weight (g/mol).
[b] LogP, octanol/water partition coefficient.
[c] OHNH donors, number of protons able to act as hydrogen bond donors.
[d] ON acceptors, number of protons capable of acting as hydrogen bond acceptors.
[f] GI absorption, human intestinal absorption.
[g] Water solubility, amount of the compound that dissolves in water.
[h] Caco-2, apparent permeability of the Caco-2 cell.

4. Materials and methods

4.1. Chemistry

Fig. 2 illustrates the synthetic process carried out to obtain the selenocyanate derivatives (Series A) and the diselenides (Series B). Intermediates **A0** and **B0** were synthesized according to a method previously described [28]. The reagents were commercially available. Melting points (Mp) were determined with a Mettler FP82 + FP80 (Greifensee, Switzerland). Reactions were monitored by thin-layer chromatography (TLC) and spots were visualized under UV light. ^{1}H,^{13}C and ^{77}Se-NMR spectra were registered on a Bruker Avance Neo 400 MHz operating at 400, 100 and 76 MHz, respectively, in $CDCl_3$ or DMSO-d_6.

4.1.1. General procedure for the preparation of selenocyanate derivatives (A1-10)

The synthesis of selenocyanate derivatives (**A1-10**) was carried out following a reported experimental procedure [28] [1]. In particular, intermediate 4-aminophenyl selenocyanate (**A0**) was obtained by reaction of selenium dioxide (6 mmol), malononitrile (3 mmol) and aniline (4.5 mmol) in 15 mL of dimethylsulfoxide (DMSO) for 1 h. Afterwards, the reaction crude was added over cold water (150 mL) and was isolated by filtration and purified after several washes with *n*-hexane (5 × 15 mL). The intermediate **A0** (5 mmol) was reacted with different acid chlorides (5 mmol) and potassium carbonate (15 mmol) using 50 mL of dichloromethane (DCM) as solvent for 24 h. After that, the solvent was removed under reduced pressure and the crude was washed with water (50 mL). Then, the derivatives of this series were isolated by filtration and purified by washing with *n*-hexane.

***N*-(4-selenocyanatophenyl) pentanamide (A1).** From: 4-selenocyanates aniline and pentoyl chloride. Appearance: brown solid. Melting point: 150 °C. Yield: 32%. ^{1}H NMR (400 MHz, $CDCl_3$) δ 1.00 (t, J = 7.4 Hz, 3H, Alif), 1.75 (m, 2H, Alif), 2.35 (t, J = 7.8 Hz, 2H, Alif), 7.50 (s, 1H, NH), 7.59 (s, 4H, Aryl). ^{13}C NMR (101 MHz, $CDCl_3$) δ 13.73, 18.91, 39.61, 101.96 (C-Se), 115.01, 121.16, 134.63, 140.04, 171.70 (C═O). ^{77}Se NMR (76 MHz, $CDCl_3$) δ 314.20. Anal. Calcd for $C_{11}H_{12}N_2OSe$ (%): C, 49.45; H, 4.53; N, 10.48. Found: C, 49.23; H, 4.62; N, 11.22.

***N*-(4-selenocyanatophenyl) butyramide (A2).** From: 4-selenocyanateaniline and butyryl chloride. Appearance: Yellow cottony solid. Mp: 105 °C. Yield: 21%. ^{1}H NMR (400 MHz, $CDCl_3$) δ 0.95 (t, J = 7.3 Hz, 3H, Alif), 1.41 (m, 2H, Alif), 1.71 (p, J = 7.6 Hz, 2H, Alif), 2.37 (t, J = 7.6 Hz, 2H, Alif), 7.40 (s, 1H, NH), 7.59 (s, 4H, Aryl). ^{13}C NMR (101 MHz, $CDCl_3$) δ 13.80, 22.36, 27.50, 37.53, 101.81 (C-Se), 115.07, 121.11, 134.64, 139.99, 171.71 (C═O). ^{77}Se NMR (76 MHz, $CDCl_3$) δ 313.69. Anal. Calcd for $C_{12}H_{14}N_2OSe$ (%): C, 51.25; H, 5.02; N, 9.96. Found: C, 51.40; H, 5.10; N, 9.46.

***N*-(4-selenocyanatophenyl) heptanamide (A3).** From: 4-selenocyanateaniline and caproyl chloride. Appearance: brown solid. Mp: 111 °C. Yield: 12%. ^{1}H NMR (400 MHz, $CDCl_3$) δ 0.92 (m, 3H, Alif), 1.36 (m, 4H, Alif), 1.73 (m, 2H, Alif), 2.37 (t, J = 7.6 Hz, 2H, Alif), 7.32 (s, 1H, NH), 7.60 (s, 4H, Aryl). ^{13}C NMR (101 MHz, $CDCl_3$) δ 13.93, 22.41, 25.12, 31.38, 37.79, 101.72 (C-Se), 121.09, 134.64, 134.64, 139.95, 171.66 (C═O). ^{77}Se NMR (76 MHz, $CDCl_3$) δ 313.75. Anal. Calcd for $C_{13}H_{16}N_2OSe$ (%): C, 52.88; H, 5.46; N, 9.49. Found: C, 52.48; H, 5.66; N, 9.69.

***N*-(4-selenocyanatophenyl) undecanamide (A4).** From: 4-selenocyanateaniline and capric chloride. Appearance: beige solid. Mp: 104 °C. Yield: 57%. 104 °C. ^{1}H NMR (400 MHz, $CDCl_3$) δ 0.88 (m, 3H, Alif), 1.29 (m, 12H, Alif), 1.72 (p, J = 7.5 Hz, 2H, Alif), 2.37 (t, J = 7.6 Hz, 2H, Alif), 7.38 (s, 1H, NH), 7.59 (s, 4H, Aryl). ^{13}C NMR (101 MHz, $CDCl_3$) δ 14.11, 22.67, 25.45, 29.24, 29.27, 29.36, 29.43, 31.86, 37.84, 101.73 (C-Se), 121.09, 134.63, 139.96, 171.67 (C═O). ^{77}Se NMR (76 MHz, $CDCl_3$) δ 313.76. Anal. Calcd for $C_{17}H_{24}N_2OSe$ (%): C, 58.11; H, 6.89; N, 7.97. Found: C, 58.23; H, 6.58; N, 7.70.

***N*-(4-selenocyanatophenyl) dodecanamide (A5).** From: 4-selenocyanateaniline and lauroyl chloride. Appearance: white solid. Mp: 109%. Yield: 9%. ^{1}H NMR (400 MHz, $CDCl_3$) δ 0.88 (t, J = 6.7 Hz, 3H, Alif), 1.27 (m, 16H, Alif), 1.72 (p, J = 7.4 Hz, 2H, Alif), 2.37 (t, J = 7.6 Hz, 2H, Alif), 7.25 (s, 1H, NH), 7.60 (s, 4H, Aryl). ^{13}C NMR (101 MHz, $CDCl_3$) δ 22.69, 25.46, 29.25, 29.34, 29.37, 29.48, 29.61, 29.62, 31.91, 37.81, 101.87 (C-Se), 115.02, 121.13, 134.62, 140.02, 171.79. ^{77}Se NMR (76 MHz, $CDCl_3$) δ 313.64. Anal. Calcd for $C_{19}H_{28}N_2OSe$ (%): C, 60.15; H, 7.44; N, 7.38. Found: C, 60.25; H, 7.81; N, 7.46.

***N*-(4-selenocyanatophenyl) palmitamide (A6).** From: 4-selenocyanateaniline and palmitoyl chloride. Appearance: brown solid. Mp: 97 °C. Yield: 10%. ^{1}H NMR (400 MHz, $CDCl_3$) δ 0.88 (t, J = 6.7 Hz, 3H, Alif), 1.25 (s, 24H, Alif), 1.71 (p, J = 7.4 Hz, 2H, Alif), 2.36 (t, J = 7.6 Hz, 2H, Alif), 7.58 (d, J = 8.8 Hz, 2H, Aryl), 7.66 (d, J = 8.5 Hz, 2H, Aryl), 8.38 (s, 1H, NH). ^{13}C NMR (101 MHz, $CDCl_3$) δ 13.92, 22.48, 27.62, 37.66, 101.92 (C-Se), 115.21, 121.24, 134.77, 134.83, 140.11, 171.83 (C═O). ^{77}Se NMR (76 MHz, $CDCl_3$) δ 313.76. Anal. Calcd for $C_{23}H_{36}N_2OSe$ (%): C, 63.43; H, 8.33; N, 6.43. Found: C, 63.63; H, 8.11; N, 6.37.

***N*-(4-selenocyanatophenyl) cyclopropanecarboxamide (A7).** From: 4-selenocyanateaniline and cylopropanecarbonyl chloride. Appearance: brown solid. Mp: 150 °C. Yield: 86%. ^{1}H NMR (400 MHz, $CDCl_3$) δ 0.89 (m, 2H, Alif), 1.11 (m, 2H, Alif), 1.52 (m, 1H, Alif), 7.56 (s, 1H, NH), 7.59 (s, 4H, Alif). ^{13}C NMR (101 MHz, Chloroform-*d*) δ 8.41, 15.80, 102.00 (C-Se), 114.81, 121.09, 134.67, 140.18, 172.37 (C═O). ^{77}Se NMR (76 MHz, $CDCl_3$δ 313.68. Anal. Calcd for $C_{11}H_{10}N_2OSe$ (%): C, 49.82; H, 3.80; N, 10.56. Found: C, 49.56; H, 3.94; N, 10.72.

***N*-(4-selenocyanatophenyl) cyclobutanecarboxamide (A8).** From: 4-selenocyanateaniline and cyclobutanecarbonyl chloride. Appearance: reddish solid. Mp: 145 °C. Yield: 60%. ^{1}H NMR (400 MHz, $CDCl_3$) δ 1.62 (m, 2H, Alif), 1.77 (m, 2H, Alif), 1.89 (m, 3H, Alif), 2.69 (p, J = 8.0 Hz, 1H, Alif), 7.58 (m, 4H, Aryl). ^{13}C NMR (101 MHz, $CDCl_3$) δ 18.04, 25.25, 40.85, 101.77 (C-Se), 121.04, 134.67, 140.05, 173.48 (C═O). ^{77}Se NMR (76 MHz, $CDCl_3$) δ 313.94. Anal. Calcd for $C_{12}H_{12}N_2OSe$ (%): C, 51.62; H, 4.33; N, 10.03. Found: C, 51.41; H, 4.68; N, 10.28.

***N*-(4-selenocyanatophenyl) cyclopentanecarboxamide (A9).** From: 4-selenocyanateaniline and cyclopentanecarbonyl chloride. Appearance: solid brown. Mp: 131 °C. Yield: 36%. ^{1}H NMR (400 MHz, $CDCl_3$) δ 1.64 (m, 2H, Alif), 1.79 (m, 2H, Alif), 1.90 (m, 4H, Alif), 2.69 (p, J = 8.0 Hz, 1H, Alif), 7.52 (s, 1H, NH), 7.58 (s, 4H, Aryl). ^{13}C NMR (101 MHz, $CDCl_3$) δ 26.03, 30.50, 46.90, 101.77 (C-Se), 114.93, 121.05, 134.65, 140.16, 174.89 (C═O). ^{77}Se NMR (76 MHz, $CDCl_3$) δ 313.63. Anal. Calcd for $C_{13}H_{14}N_2OSe$ (%): C, 53.25; H, 4.81; N, 9.55 Found: C, 52.98; H, 4.58; N, 9.48.

***N*-(4-selenocyanatophenyl) cyclohexanecarboxamide (A10).** From: 4-selenocyanateaniline and cyclohexanecarbonyl chloride. Appearance: beige solid. Mp: 136 °C. Yield: 44%. ^{1}H NMR (400 MHz, $CDCl_3$) δ 1.30 (m, 4H, Alif), 1.54 (m, 12.1 Hz, 3H, Alif), 1.72 (m, 1H, Alif), 1.85 (m, 2H, Alif), 1.96 (m, 2H, Alif), 2.24 (m, 1H, Alif), 7.33 (s, 1H, NH), 7.60 (s, 4H, Aryl). ^{13}C NMR (101 MHz, $CDCl_3$) δ 25.60, 29.59, 46.59, 101.69 (C-Se), 121.11, 134.64, 140.08, 174.58 (C═O). ^{77}Se NMR (76 MHz, $CDCl_3$) δ 313.51. Anal. Calcd for $C_{14}H_{16}N_2OSe$ (%): C, 54.73; H, 5.25; N, 9.12. Found: C, 54.49; H, 5.10; N, 9.36.

*4.1.2. General procedure for the preparation of diselenides derivatives (**B1-10**)*

Derivatives of series II were obtained using two synthetic procedures. For compounds **B1-4**, the intermediate **B0** (1 mmol) was obtained as a result of the reaction between the intermediate **B0** (5 mmol) with different acid chlorides (5 mmol) and potassium carbonate (15 mmol) using 50 mL of dichloromethane (DCM) as solvent for 24 h. After that, the solvent was removed under reduced pressure and the crude was washed with water (50 mL). Then, the derivatives of this series were isolated by filtration and purified by washing with *n*-hexane. Finally, derivatives **B7-10** were obtained by reduction of their corresponding selenocyanates (**A7-10**) with sodium borohydride (0.25 mmol) in ethanol (30 mL) overnight. After that, the solvent was removed under reduced pressure and the crude was washed with water (50 mL). Then, the derivatives of this series were isolated by filtration and purified by washing with *n*-hexane. Spectroscopic characterization of compounds **B5** and **B6** was not posible, due to solubility problems.

***N,N*'-(diselanediylbis(4,1-phenylene))dipentanamide (B1).** From: 4,4-diselenediyldianiline and pentoyl chloride. Appearance: green solid. Mp: 155 °C. Yield: 29%. ^{1}H NMR (400 MHz, DMSO-d_6) δ 0.91 (t, J = 7.4 Hz, 6H, Alif), 1.61 (h, J = 7.4 Hz, 4H, Alif), 2.29 (t, J = 7.3 Hz, 4H, Alif), 7.55 (dd, J = 8.93, 8.85 Hz, 8H, Aryl), 10.00 (s, 2H, NH). ^{13}C NMR (101 MHz, DMSO-d_6) δ 14.08, 18.97, 38.81, 120.23, 123.84, 133.67, 140.13, 171.81 (C═O). ^{77}Se NMR (76 MHz, DMSO-d_6) δ 480.41. Anal. Calcd for $C_{20}H_{24}N_2O_2Se_2$ (%): C, 49.80; H, 5.02; N, 5.81. Found: C, 50.09; H, 4.86; N, 5.63.

***N,N*'-(diselanediylbis(4,1-phenylene))dibutyramide (B2).** From: 4,4-diselenediyldianiline and butyryl chloride. Appearance: yellow solid. Mp: 164 °C. Yield: 31%. ^{1}H NMR (400 MHz, DMSO-d_6) δ 0.89 (d, J = 7.3 Hz, 6H, Alif), 1.31 (m, 4H, Alif), 1.56 (m, 4H, Alif), 2.30 (d, J = 7.5 Hz, 4H, Alif), 7.54 (dd, J = 8.0, 8.8 Hz, 8H, Aryl), 9.99 (s, 1H, NH). ^{13}C NMR (101 MHz, DMSO-d_6) δ 14.20, 22.28, 27.66, 36.62, 120.22, 123.83, 133.67, 140.14, 171.95 (C═O). ^{77}Se NMR (76 MHz, DMSO-d_6) δ 480.54. Anal. Calcd for $C_{22}H_{28}N_2O_2Se_2$ (%): C, 51.77; H, 5.53; N, 5.49. Found: C, 52.01; H, 5.24; N, 5.66.

***N,N*'-(diselanediylbis(4,1-phenylene))dihexanamide (B3).** From: 4,4-diselenediyldianiline and caproyl chloride. Appearance: yellow solid. Mp: 154 °C. Yield: 24%. ^{1}H NMR (400 MHz, DMSO-d_6) δ 0.91 (d, J = 7.3 Hz, 6H, Alif), 1.61 (m, 4H, Alif), 2.29 (m, 4H, Alif), 7.55 (dd, J = 8.93, 8.85 Hz, 8H, Aryl), 10.00 (s, 2H, NH).NMR (400 MHz, DMSO-d_6) δ 0.87 (t, J = 6.7 Hz, 6H, Alif), 1.30 (m, 6H, Alif), 1.59 (m, 4H, Alif), 2.30 (t, J = 7.4 Hz, 4H, Alif), 7.54 (dd, J = 8.1, 8.4 Hz, 8H, Aryl), 9.99 (s, 2H, NH). ^{13}C NMR (101 MHz, DMSO-d_6) δ 14.34, 22.37, 25.21, 31.35, 36.87, 120.22, 123.84, 133.67, 140.14, 171.95 (C═O). ^{77}Se NMR (76 MHz, DMSO-d_6) δ 480.41. Anal. Calcd for $C_{24}H_{32}N_2O_2Se_2$ (%): C, 53.53; H, 5.99; N, 5.20. Found: C, 53.78; H, 5.24; N, 5.66.

***N,N*'-(diselanediylbis(4,1-phenylene))bis(decanamide) (B4).** From: 4,4-diselenediyldianiline and capric chloride. Appearance: yellow solid. Mp: 170 °C. Yield: 67%. ^{1}H NMR (400 MHz, DMSO-d_6) δ 0.85 (t, 6H, Alif), 1.25 (m, 23H, Alif), 1.57 (t, J = 7.2 Hz, 2H, Alif), 2.29 (t, J = 7.4 Hz, 4H, Alif), 7.53 (dd, J = 7.90, 8.06 Hz, 8H, Aryl), 9.99 (s, 2H, NH). ^{13}C NMR (101 MHz, DMSO-d_6) δ 14.42, 22.57, 25.53, 29.13, 29.15, 29.28, 29.37, 31.75, 36.90, 120.20, 123.80, 133.64, 140.17, 171.94 (C═O). ^{77}Se NMR (76 MHz, DMSO-d_6) δ 480.86. Anal. Calcd for $C_{32}H_{48}N_2O_2Se_2$ (%): C, 59.07; H, 7.44; N, 4.31. Found: C, 53.78; H, 5.24; N, 5.66.

***N,N*'-(diselanediylbis(4,1-phenylene))dicyclopropanecarboxamide (B7).** From: 4-selenocyanateaniline and cyclopropanecarbonyl chloride. Appearance: yellow solid. Mp: 207 °C. Yield: 12%. ^{1}H NMR (400 MHz, DMSO-d_6) δ 0.81 (m, 8H, Alif), 1.79 (m, 2H, Alif), 7.54 (dd, J = 8.0, 8.6 Hz, 8H, Aryl), 10.38 (s, 2H, NH). ^{13}C NMR (101 MHz, DMSO-d_6) δ 7.79, 15.05, 120.20, 133.72, 140.18, 172.32 (C═O). ^{77}Se NMR (76 MHz, DMSO-d_6) δ 480.82. ^{77}Se NMR (76 MHz, DMSO-d_6) δ 480.82. Anal. Calcd for $C_{20}H_{20}N_2O_2Se_2$ (%): C, 50.22; H, 4.21; N, 5.86. Found: C, 50.48; H, 4.41; N, 5.89.

***N,N*'-(diselanediylbis(4,1-phenylene))dicyclobutanecarboxamide (B8).** From: 4-selenocyanateaniline and cyclobutanecarbonyl chloride. Appearance: yellow solid. Mp: 187 °C. Yield: 65%.^{1}H NMR (400 MHz, DMSO-d_6) δ 1.56 (m, 4H, Alif), 1.70 (m, 8H, Alif), 1.84 (m, 4H, Alif), 7.54 (dd, J = 8.8, 9.0 Hz, 8H, Aryl), 9.99 (s, 2H, NH). ^{13}C NMR (101 MHz, DMSO-d_6) δ 18.18, 25.04, 120.30, 123.82, 133.66, 140.17, 173.54 (C═O). ^{77}Se NMR (76 MHz, DMSO-d_6) δ 480.73. Anal. Calcd for $C_{22}H_{24}N_2O_2Se_2$ (%): C, 52.18; H, 4.78; N, 5.53. Found: C, 51.96; H, 4.91; N, 5.46.

***N,N*'-(diselanediylbis(4,1-phenylene))dicyclopentanecarboxamide (B9).** From: 4-selenocyanateaniline and cyclopentanecarbonyl chloride. Appearance: yellow solid. Mp: 188 °C. Yield: 67%. ^{1}H NMR (400 MHz, DMSO-d_6) δ 1.56 (m, 4H), 1.70 (m, 8H), 1.84 (m, 4H), 7.54 (dd, J = 8.8, 9.0 Hz, 8H), 9.99 (s, 2H). ^{13}C NMR (101 MHz, DMSO-d_6) δ 26.10, 30.49, 45.74, 120.24, 133.66, 140.24, 175.01 (C═O). ^{77}Se NMR (76 MHz, DMSO-d_6) δ 481.33. Anal. Calcd for $C_{24}H_{28}N_2O_2Se_2$ (%): C, 53.94; H, 5.28; N, 5.24. Found: C, 54.09; H, 5.33; N, 5.15.

***N,N*'-(diselanediylbis(4,1-phenylene))dicyclohexanecarboxamide (B10).** From: 4-selenocyanateaniline and cyclohexanecarbonyl chloride. Appearance: yellow solid. Mp: 211 °C. Yield: 57^{1}H NMR (400 MHz, DMSO-d_6) δ 1.23 (m, 6H), 1.40 (m, 4H), 1.65 (d, J = 10.9 Hz, 2H), 1.77 (m, 8H), 2.32 (m, 2H), 7.54 (dd, J = 8.3, 8.7 Hz, 8H), 9.94 (s, 2H). ^{13}C NMR (101 MHz, DMSO-d_6) δ 25.68, 29.55, 45.34, 120.25, 123.77, 133.69, 140.31, 174.96 (C═O). ^{77}Se NMR (76 MHz, DMSO-d_6) δ 481.68. Anal. Calcd for $C_{26}H_{32}N_2O_2Se_2$ (%): C, 55.52; H, 5.73; N, 4.98. Found: C, 55.71; H, 5.84; N, 4.86.

4.2. Biology

4.2.1. Parasite culture

Promastigotes. L. major (clone VI, MHOM/IL/80) and *L. infantum* (clone, BCN-150) parasites were grown at 26 °C under continuous shaking in M199 1X medium (Sigma, St Louis, MO, USA) supplemented with heat-inactivated fetal bovine serum (FBS), 25 mM HEPES (pH 7), 0.1 mM adenine, 0.0005% (w/v) haemin, 0.0001% (w/v), 0.0005% (w/v) biotin, 100 IU/mL penicillin and 100 mg/mL streptomycin. Before each experiment, medium was changed to ensure that parasites were in an exponential growth phase. For infections, stationary promastigotes were cultured in modified Schneider's medium at 26 °C under continuous shaking supplemented with 20% FBS, 100 IU/mL penicillin and 100 mg/mL streptomycin for 5–6 days.

Axenic amastigotes. Axenic parasites of *L. infantum* were cultured in M199 medium (Invitrogen, Leiden, The Netherlands) supplemented with 10% heat-inactivated FBS, 1 g alanine, 100 mg L-asparagine, 200 mg sucrose, 50 mg sodium pyruvate, 320 mg malic acid, 40 mg fumaric acid, 70 mg succinic acid, 200 mg ketoglutaric acid, 300 mg citric acid, 1.1 g sodium bicarbonate, 5 g morpholinoethanesulphonic acid (MES), 0.4 mg haemin, 10 mg gentamicin at pH 5.4 at 37 °C and 5% CO_2.

4.2.2. Cell culture

Human monocytic leukaemia cell line THP-1. THP-1 cells were cultured in RMPI 1640 medium (Gibco, Leiden, The Netherlands) supplemented with 10% heat-inactivated FBS, 5% penicillin/streptomycin, 1 mM HEPES, 2 mM glutamine at pH 7.2 at 37 °C and 5% CO_2.

Bone marrow derived macrophages (BMDM). BMDM were obtained after rinsing the femur and tibia with phosphate-buffered saline (PBS, Gibco, Gaithersburg, MD, USA). The monocytes were then resuspended in Dulbecco's modified Eagle's medium (DMEM, Gibco, Gaithersburg, MD, USA) supplemented with 10% FBS, 1% penicillin/streptomycin and 20% filtered supernatant from the L929 cell line (obtained from the ATCC collection) as a source for granulocyte–macrophage colony-stimulating factor (GM-CSF), required to stimulate the differentiation of hematopoietic cells into macrophages. Therefore, the cells were incubated for 8 days at 37 °C and 5% CO_2 and the culture medium were changed every 3 days.

4.2.3. Animals

BALB/c mice were maintained under standardized conditions of free access to food and water. They were stored in groups in plastic cages under controlled environmental conditions (12/12 h of light/dark cycle and 22 ± 2 °C). Following the ethical standards approved by the Animal Ethics Committee of the University of Navarra in accordance with the European legislation.

4.2.4. Leishmanicidal activity of Se-compounds against promastigotes

To determine the antileishmanial activity of the compounds, promastigotes of *L. major* and *L. infantum* (3×10^5 promastigotes/100 μL) were seeded in 96-well plates and were treated with increasing concentrations of the compounds (1–500 μM) diluted in supplemented M199 1x medium and maintained at 26 ∘C for 48 h. After 48 h, the MTT assay was performed. Briefly, 20 μL/well of MTT (5 mg/mL in PBS) was added and incubated for 4 h under the same conditions. Then, 80 μL of DMSO was added to each well to dissolve formazan crystals. The absorbance was measured on a Multiskan EX photometric plate reader for microplates at 540 nm. Data were obtained from three independent experiments performed in triplicate. The effective concentration values (EC_{50}) were obtained by fitting the data to a dose–inhibition sigmoid curve using GraphPad Prism 7.0 software (GraphPad Software Inc., San Diego, CA, USA). MIL and PMN were used as reference drugs for comparison.

4.2.5. Drug combination studies

The fractional inhibitory concentration index (FICI) was used to describe the interaction between the lead compounds B8 and B9 with AmB, PMN and MIL *in vitro* against *Leishmania* promastigotes after 48 h of treatment. For that purpose, starting from the EC_{50} of each compound, two higher concentrations ($EC_{50} \times 2$ and $EC_{50} \times 4$) and two lower concentrations (EC_{50} / 2 and IC_{50} / 4) were set. After 48 h, the MTT assay was performed, as described above. For each combination, FICI was calculated according to the formula: FICA = EC50 of compound A in combination with compound B / EC50 of compound A alone; FICB = EC_{50} of compound B in combination with compound A / EC_{50} of compound B alone. Then, the sum of all FICs (SFIC) for each combination was calculated (SFIC = FIC compound A + FIC compound B). Finally, the FICI value was calculated (SFIC divided by de number of the different combinations). FICI was used to describe the compound interaction effects *in vitro*. Synergy was defined as FICI < 0.5, no-interaction as 0.5 < FICI < 4, and antagonism as FICI > 4 [37]. FICI values were obtained from three independent experiments.

4.2.6. Leishmanicidal activity of Se-compounds against amastigotes cytotoxicity studies

THP-1 and BMDM cytotoxicity. THP-1 cells were seeded at a concentration of 8×10^4 cells/mL in 96-well plates and differentiated to macrophages with phorbol 12-myristate 13-acetate (PMA) (10 ng/mL) for 24 h in supplemented RPMI1640 medium (Gibco, Leiden, The Netherlands) at 37 °C and 5% CO_2. In the case of the lead compounds, BMDM were seeded at the same concentration in supplemented DMEM medium. After 24 h, the culture medium was removed and cells were treated with the synthetized compounds at different concentrations ranging from 1 to 500 μM and incubated for 48 h. After this time, the MTT assay was performed. The absorbance was measured on a MultiskanEX photometric plate reader for microplates at 540 nm. Data were obtained from three independent experiments performed in triplicate. The cytotoxic concentration values (CC50) were obtained by fitting the data to a dose–inhibition sigmoid curve using GraphPad Prism 7.0 software (GraphPad Software Inc., San Diego, CA, USA). MIL and PMN were used as reference drugs for comparison.

Axenic amastigotes assay. Axenic amastigotes of *L. infantum* were seeded in 96-well plates at a concentration of 1×10^6 parasites/mL and compounds were added. Parasites were kept in incubation at 26 °C for 24 h with the lead drugs. The number and percentage of living parasites was figured out by flow cytometry by the propidium iodide (PI) exclusion method, as previously described [27]. All assays were performed with a minimum of three independent experiments. The effective concentration values (EC_{50}) were obtained by fitting the data to a dose–inhibition sigmoid curve using GraFit 6 software (Erithacus, Horley, Surrey, UK).

Back transformation assay (BTA). The activity of the lead compounds was assessed against *L. major* and *L. infantum* amastigotes by the BTA assay after 48 h. BMDM were seeded at 8×10^4 cell/well in 96-well plates and incubated at 37 °C for 24 h in supplemented DMEM medium. Cells were then infected with *L. major* or *L. infantum* stationary promastigotes in a 10:1 ratio (parasite:macrophage) and incubated with parasites overnight at 37 °C and 5% CO_2. In the case of *L. major* parasites, metacyclic promastigotes were isolated by the peanut agglutinin (PNA) method. Afterwards, cells were washed with PBS and treated with different concentrations of compounds for 48 h. Then, medium was removed and infected cells were incubated at 26 °C in modified Schneider's complete medium (20% FBS) to promote the release of the remaining viable amastigotes. At the end of 5–7 days, remaining parasites were transferred to new 96-well plates and the MTT assay was performed [41,42]. EC_{50} values were determined by fitting the data to a dose–inhibition sigmoid curve using GraphPad Prism 7.0 software (GraphPad Software Inc., San Diego, CA, USA). Selectivity (SI) was calculated as the ratio between the CC_{50} values of the compounds against BMDM and the EC_{50} values obtained in *Leishmania* amastigotes.

Giemsa staining assay. BMDM (8×10^4 cells/well) were seeded in 8-well culture chamber slides (Lab-TekTM, BD Biosciences) in supplemented DMEM medium and allowed to adhere for 24 h at 37 °C in a 5% CO_2 incubator. In the case of *L. major* parasites, metacyclic promastigotes were isolated by the peanut agglutinin (PNA) method. *L. infantum* and *L. major* promastigotes were added to wells at a macrophage/parasite ratio of 1:10. LabTek chambers were incubated for 24 h to allow infection. After infection, wells were washed with PBS to remove unphagocytosed parasites and treated for 48 h with lead compounds at different concentrations.After this time, the supernatant was removed and cells were washed with PBS, fixed with cold methanol and stained with Giemsa. The percentage of infected macrophages and the number of amastigotes per 100 macrophages were evaluated by counting 200 macrophages using an optical microscope (Nikon Eclipse E400). The experiment was performed three times in duplicate wells and results are presented as EC_{50} mean ± SD. The selectivity index (SI) was calculated as the ratio between cytotoxicity (CC_{50}) against BMDM and effectivity (EC_{50}) against *Leishmania* amastigotes.

4.2.7. Studies of the mechanism of action

TryR inhibition assay. To determine the oxidoreductase activity of the TryR enzyme, the procedure described by Toro *et. al.* [57] was used. For this purpose, reactions were conducted at 26 ∘C in 250 μL of a buffer containing 40 mM HEPES pH 7.5, 1 mM EDTA, 30 μM $NADP^+$, 25 μM

DTNB, 1 μM TS_2, 150 μM NADPH, 0.02% glycerol, 1.75% DMSO and 7 nM recombinant LiTryR. TryR oxidoreductase activity was monitored at 26 ∘C by the increase in absorbance at 412 nm due to TNB generation in an EnSpire Multimode Plate Reader (PerkinElmer, Waltham, MA). IC_{50} values for each compound were obtained by fitting these percentages to a nonlinear regression model with the GraFit 6 software (Erithacus, Horley, Surrey, UK). All the assays were conducted in three independent experiments.

IC_{50} values were determined using the two-parameter IC_{50} equation provided by GraFit, where the lower data limit is 0%, and the upper limit is 100%:

$$y = \frac{100}{1 + \left(\frac{x}{IC_{50}}\right)^{s}} \quad (1)$$

The reciprocal value of the initial reaction rates of TryR reaction progress curves at different **B8** and TS_2 concentrations were fitted to the reciprocal equation that describes competitive inhibition:

$$\frac{1}{v} = \frac{1}{V_{max}} + \left(\frac{1}{[S]}\frac{K_m}{V_{max}}\right)\left(1 + \frac{[I]}{K_i}\right) \quad (2)$$

*Reversibility of TryR inhibition by **B8***. The reversibility of TryR inactivation by **B8** was assessed by measuring the oxidoreductase activity of extensively diluted samples of the enzyme preincubated with or without inhibitor. TryR (400 nM) was incubated with 25 μM **B8** or the vehicle (DMSO) in a buffer containing 40 mM HEPES pH 7.5 and 1 mM EDTA during 16 h. Once preincubations were complete, all samples were diluted with a buffer containing HEPES (pH 7.5, 40 mM) and EDTA (1 mM) and subsequently distributed (6.25 μL) in a 96-well microplate. All reactions were initiated at the same time by addition of 243.75 μL of an activity buffer containing HEPES (pH 7.5, 40 mM), EDTA (1 mM), NADP+ (61.54 μM), DTNB (153.85 μM), NADPH (307.69 μM) and TS_2 (102.56 μM). The final assay mixtures (250 μL) contained HEPES (pH 7.5, 40 mM), EDTA (1 mM), NADPH (300 μM), $NADP^+$ (60 μM), DTNB (25 μM), TS_2 (100 μM), and recombinant TryR (1 nM) with or without 62.5 nM **B8**. Enzyme activity was monitored at 26 °C through the increase in absorbance at 412 nm in an EnSpire Multimode Plate Reader (PerkinElmer, Waltham, MA, USA). 2-nitro-5-mercaptobenzoic acid (TNB) concentration was obtained by multiplying the absorbance values by 100 (50 μM TNB generates 0.5 arbitrary units of absorbance at 412 nm). In this DTNB-coupled assay, one molecule of $T[SH]_2$ reduces one molecule of DTNB, producing two TNB molecules. All assays were conducted in triplicate in at least three independent experiments. In these experiments TryR was also preincubated with 25 μM mepacrine as a control for a reversible inhibitor.

*Preincubation time dependence of TryR inhibition by **B8***. TryR (400 nM) was preincubated at 26 °C with increasing concentrations of **B8** or the vehicle (DMSO) during different time periods in a buffer (150 μL) containing HEPES (pH 7.5, 40 mM) and EDTA (1 mM). Once preincubations were complete, all samples were diluted with a buffer containing HEPES (pH 7.5, 40 mM) and EDTA (1 mM) and subsequently distributed (6.25 μL) in a 96-well microplate. All reactions were initiated at the same time by addition of 243.75 μL of an activity buffer containing HEPES (pH 7.5, 40 mM), EDTA (1 mM), NADP+ (61.54 μM), DTNB (153.85 μM), NADPH (307.69 μM) and TS_2 (102.56 μM). The final assay mixtures (250 μL) contained HEPES (pH 7.5, 40 mM), EDTA (1 mM), NADPH (300 μM), $NADP^+$ (60 μM), DTNB (25 μM), TS_2 (100 μM), and recombinant TryR (1 nM) with or without different concentrations of **B8** (ranging from 11.72 to 187.5 nM). Enzyme activity was monitored at 26 °C through the increase in absorbance at 412 nm in an EnSpire Multimode Plate Reader (PerkinElmer, Waltham, MA, USA). GraFit 6.0 software (Erithacus, Horley, SRY, UK) was used to fit data from three independent experiments to the following equation:

$$\frac{v_i}{v_0} = \exp(-k_{obs}t) \quad (3)$$

where v_i is the initial velocity at each inhibitor concentration, v_0 is the initial velocity in the absence of inhibitor and without preincubation, and k_{obs} is the apparent first-order rate constant for the conversion of v_i into the steady-state velocity (v_s).

The inhibition constant ($K_{i(irrev)}$) for the irreversible kinetic mechanism and the rate constant for the inactivation (k_{inact}) were determined by fitting the k_{obs} values obtained at different **B8** concentrations to Equation (4) using GraFit 6.0 software (Erithacus, Horley, SRY, UK).

$$k_{obs} = \frac{k_{inact}[I]}{K_{i(irrev)} + [I]} \quad (4)$$

Nitric oxide assay. To measure the production of NO by BMDM after the addition of the lead compounds, the Griess reaction was used [58]. Briefly, BMDM were seeded in 96-well plates at a density of 8×10^4 cells/well and allowed to adhere for 24 h at 37 °C in a humidified atmosphere with 5% CO_2. The medium was then replaced with fresh DMEM medium containing different concentrations (10, 20, 50 and 100 μM) of the selected compounds and plates were incubated for 48 h. Subsequently, 100 μL of culture supernatant were incubated with an equal volume of the Griess reagent (Panreac) (0.5% sulfanilamide and 0.05% naphthylene-diamide dihydrochloride in 2.5 % H_3PO_4) for 30 min at r.t.. Absorbance was measured using a Multiskan EX photometric plate reader for microplates at 540 nm. The concentration of nitrite in the medium was determined from the calibration curve obtained using different concentrations of sodium nitrite (Sigma, MO, USA). Three independent experiments were performed in duplicate.

Measurement of ROS production. BMDMs were seeded in 96-well microplates (8×10^4 cells/well) for 24 h at 37 °C. Compounds (10, 20, 50 and 100 μM) were added and maintained for 48 h. After this time, plates were washed with PBS and H_2DCFDA (20 μM) was added for 30 min. The reading was performed on a spectrofluorometer (485/528 nm). BMDM were used as negative control and those stimulated with H_2O_2 (4 mM) for 30 min were used as positive control. Three independent experiments were performed in duplicate.

4.2.8. Theorical ADME and Lipinski properties

Absorption, distribution, metabolism, excretion, and toxicity (ADME) parameters were calculated using pkCSM software (https://biosig.lab.uq.edu.au/pkcsm/prediction).

4.2.9. Statistical analysis

Statistical significance was analyzed using Prism 6.0 software. Differences were tested using the one-way ANOVA with Dunnetťs post hoc test for multiple comparison with * $p < 0.05$; ** $p < 0.01$; *** $p < 0.001$ and **** $p < 0.0001$.

Declaration of Competing Interest

The authors declare that they have no known competing financial interests or personal relationships that could have appeared to influence the work reported in this paper.

Data availability

Data will be made available on request.

Acknowledgements

This research was financially supported by the Plan de Investigación de la Universidad de Navarra, PIUNA (2018-19) and by the Institute of Tropical Health of University of Navarra (ISTUN), Caixa Foundation, Roviralta and Ubesol, Spain. AH-F gratefully acknowledges the support provided by the Institute of Tropical Health of University of Navarra (ISTUN) for her Ph.D. fellowship.

Appendix A. Supplementary data

Supplementary data to this article can be found online at https://doi.org/10.1016/j.bioorg.2023.106624.

References

[1] M. Díaz, et al., Synthesis and Leishmanicidal Activity of Novel Urea, Thiourea, and Selenourea Derivatives of Diselenides, Antimicrob. Agents Chemother. 63 (2019) e02200–e02218, https://doi.org/10.1128/AAC.02200-18.

[2] D. Steverding, The history of leishmaniasis, Parasit. Vectors 10 (2017) 82, https://doi.org/10.1186/s13071-017-2028-5.

[3] A. Taghipour, et al., Leishmaniasis and trace element alterations: a systematic review, Biol. Trace Elem. Res. 199 (2021) 3918–3938, https://doi.org/10.1007/s12011-020-02505-0.

[4] A. Addisu, et al., Neglected tropical diseases and the sustainable development goals: an urgent call for action from the front line, BMJ Glob. Health 4 (2019), https://doi.org/10.1136/bmjgh-2018-001334.

[5] M. Ghorbani, R. Farhoudi, Leishmaniasis in humans: drug or vaccine therapy? Drug Des. Devel. Ther. 12 (2018) 25–40, https://doi.org/10.2147/dddt.S146521.

[6] Dandugudumula, R., Fischer-Weinberger, R. & Zilberstein, D. Morphogenesis Dynamics in Leishmania Differentiation. Pathogens 11, doi:10.3390/pathogens11090952 (2022).

[7] R. Olekhnovitch, P. Bousso, Induction, Propagation, and Activity of Host Nitric Oxide: Lessons from Leishmania Infection, Trends Parasitol. 31 (2015) 653–664, https://doi.org/10.1016/j.pt.2015.08.001.

[8] M.S. Gurel, B. Tekin, S. Uzun, Cutaneous leishmaniasis: A great imitator, Clin. Dermatol. 38 (2020) 140–151, https://doi.org/10.1016/j.clindermatol.2019.10.008.

[9] J. van Griensven, E. Diro, Visceral Leishmaniasis: Recent Advances in Diagnostics and Treatment Regimens, Infect. Dis. Clin. North Am. 33 (2019) 79–99, https://doi.org/10.1016/j.idc.2018.10.005.

[10] Abadías-Granado, I., Diago, A., Cerro, P. A., Palma-Ruiz, A. M. & Gilaberte, Y. Cutaneous and Mucocutaneous Leishmaniasis. Actas Dermosifiliogr (Engl Ed), doi:10.1016/j.ad.2021.02.008 (2021).

[11] S. Kumari, et al., Amphotericin B: A drug of choice for Visceral Leishmaniasis, Acta Trop. 235 (2022), https://doi.org/10.1016/j.actatropica.2022.106661.

[12] S. Palić, J.H. Beijnen, T.P.C. Dorlo, An update on the clinical pharmacology of miltefosine in the treatment of leishmaniasis, Int. J. Antimicrob. Agents 59 (2022), https://doi.org/10.1016/j.ijantimicag.2021.106459.

[13] P. Pokharel, R. Ghimire, P. Lamichhane, Efficacy and Safety of Paromomycin for Visceral Leishmaniasis: A Systematic Review, J. Trop. Med. 2021 (2021) 8629039, https://doi.org/10.1155/2021/8629039.

[14] A. Ponte-Sucre, et al., Drug resistance and treatment failure in leishmaniasis: A 21st century challenge, PLoS Negl. Trop. Dis. 11 (2017), https://doi.org/10.1371/journal.pntd.0006052.

[15] M.P. Rayman, Selenium intake, status, and health: a complex relationship, Hormones (Athens) 19 (2020) 9–14, https://doi.org/10.1007/s42000-019-00125-5.

[16] A. Cassago, et al., Identification of Leishmania selenoproteins and SECIS element, Mol. Biochem. Parasitol. 149 (2006) 128–134, https://doi.org/10.1016/j.molbiopara.2006.05.002.

[17] S. Rashidi, et al., Selenium and protozoan parasitic infections: selenocompounds and selenoproteins potential, Parasitol. Res. 121 (2022) 49–62, https://doi.org/10.1007/s00436-021-07400-8.

[18] J.C. Avery, P.R. Hoffmann, Selenium, Selenoproteins, and Immunity, Nutrients 10 (2018), https://doi.org/10.3390/nu10091203.

[19] S.A. Sculaccio, et al., Selenocysteine incorporation in Kinetoplastid: selenophosphate synthetase (SELD) from Leishmania major and Trypanosoma brucei, Mol. Biochem. Parasitol. 162 (2008) 165–171, https://doi.org/10.1016/j.molbiopara.2008.08.009.

[20] M. Bonilla, E. Krull, F. Irigoin, G. Salinas, M.A. Comini, Selenoproteins of African trypanosomes are dispensable for parasite survival in a mammalian host, Mol. Biochem. Parasitol. 206 (2016) 13–19, https://doi.org/10.1016/j.molbiopara.2016.03.002.

[21] A. Henriquez-Figuereo, C. Morán-Serradilla, E. Angulo-Elizari, C. Sanmartín, D. Plano, Small molecules containing chalcogen elements (S, Se, Te) as new warhead to fight neglected tropical diseases, Eur. J. Med. Chem. 246 (2023), https://doi.org/10.1016/j.ejmech.2022.115002.

[22] V. Alcolea, et al., 3,5-Dimethyl-4-isoxazoyl selenocyanate as promising agent for the treatment of Leishmania infantum-infected mice, Acta Trop. 215 (2021), https://doi.org/10.1016/j.actatropica.2020.105801.

[23] M. Etxebeste-Mitxeltorena, et al., Oral Efficacy of a Diselenide Compound Loaded in Nanostructured Lipid Carriers in a Murine Model of Visceral Leishmaniasis, ACS Infect. Dis. 7 (2021) 3197–3209, https://doi.org/10.1021/acsinfecdis.1c00394.

[24] Y. Baquedano, et al., Novel Heteroaryl Selenocyanates and Diselenides as Potent Antileishmanial Agents, Antimicrob. Agents Chemother. 60 (2016) 3802–3812, https://doi.org/10.1128/AAC.02529-15.

[25] P. Garnica, et al., Pre-clinical evidences of the antileishmanial effects of diselenides and selenocyanates, Bioorg. Med. Chem. Lett. 30 (2020), https://doi.org/10.1016/j.bmcl.2020.127371.

[26] M. Etxebeste-Mitxeltorena, et al., New Amides Containing Selenium as Potent Leishmanicidal Agents Targeting Trypanothione Reductase, Antimicrob. Agents Chemother. 65 (2020), https://doi.org/10.1128/AAC.00524-20.

[27] M. Etxebeste-Mitxeltorena, et al., New phosphoramidates containing selenium as leishmanicidal agents, Antimicrob. Agents Chemother. 65 (2021), https://doi.org/10.1128/AAC.00590-21.

[28] D. Plano, et al., Selenocyanates and diselenides: A new class of potent antileishmanial agents, Eur. J. Med. Chem. 46 (2011) 3315–3323, https://doi.org/10.1016/j.ejmech.2011.04.054.

[29] W. Chanput, J.J. Mes, H.J. Wichers, THP-1 cell line: an in vitro cell model for immune modulation approach, Int. Immunopharmacol. 23 (2014) 37–45, https://doi.org/10.1016/j.intimp.2014.08.002.

[30] S. Nwaka, A. Hudson, Innovative lead discovery strategies for tropical diseases, Nat. Rev. Drug Discov. 5 (2006) 941–955, https://doi.org/10.1038/nrd2144.

[31] R.V. Guido, G. Oliva, Structure-based drug discovery for tropical diseases, Curr. Top. Med. Chem. 9 (2009) 824–843, https://doi.org/10.2174/156802609789207064.

[32] K.T. Andrews, G. Fisher, T.S. Skinner-Adams, Drug repurposing and human parasitic protozoan diseases, Int. J. Parasitol. Drugs Drug Resist. 4 (2014) 95–111, https://doi.org/10.1016/j.ijpddr.2014.02.002.

[33] Y. Akao, A. Ochida, H. Muranishi, I. Nomura, T. Ichikawa, Partnership Activity for Neglected Tropical Diseases, Yakugaku Zasshi 142 (2022) 697–701, https://doi.org/10.1248/yakushi.21-00210-3.

[34] J. Utzinger, et al., Neglected tropical diseases: diagnosis, clinical management, treatment and control, Swiss Med. Wkly. 142 (2012), https://doi.org/10.4414/smw.2012.13727.

[35] I.V. Bijnsdorp, E. Giovannetti, G.J. Peters, Analysis of drug interactions, Methods Mol. Biol. 731 (2011) 421–434, https://doi.org/10.1007/978-1-61779-080-5_34.

[36] M. Gómara, S. Ramón-García, The FICI paradigm: Correcting flaws in antimicrobial in vitro synergy screens at their inception, Biochem. Pharmacol. 163 (2019) 299–307, https://doi.org/10.1016/j.bcp.2019.03.001.

[37] F.C. Odds, Synergy, antagonism, and what the chequerboard puts between them, J. Antimicrob. Chemother. 52 (2003) 1, https://doi.org/10.1093/jac/dkg301.

[38] Q.L. Fivelman, I.S. Adagu, D.C. Warhurst, Modified fixed-ratio isobologram method for studying in vitro interactions between atovaquone and proguanil or dihydroartemisinin against drug-resistant strains of Plasmodium falciparum, Antimicrob. Agents Chemother. 48 (2004) 4097–4102, https://doi.org/10.1128/aac.48.11.4097-4102.2004.

[39] G. Dias-Lopes, et al., Axenic amastigotes of Leishmania species as a suitable model for in vitro studies, Acta Trop. 220 (2021), https://doi.org/10.1016/j.actatropica.2021.105956.

[40] A.A. Abdelhaleem, E.M. Elamin, S.M. Bakheit, M.M. Mukhtar, Identification and characterization of Leishmania amastigote and axenic form antigens, Trop. Biomed. 36 (2019) 866–873.

[41] L. Maes, et al., In vitro 'time-to-kill' assay to assess the cidal activity dynamics of current reference drugs against Leishmania donovani and Leishmania infantum, J. Antimicrob. Chemother. 72 (2017) 428–430, https://doi.org/10.1093/jac/dkw409.

[42] A. Calvo, et al., Berberine-Loaded Liposomes for the Treatment of Leishmania infantum-Infected BALB/c Mice, Pharmaceutics 12 (2020), https://doi.org/10.3390/pharmaceutics12090858.

[43] S. Kumar, M.R. Ali, S. Bawa, Mini review on tricyclic compounds as an inhibitor of trypanothione reductase, J. Pharm. Bioallied Sci. 6 (2014) 222–228, https://doi.org/10.4103/0975-7406.142943.

[44] E. Weglarz-Tomczak, et al., Identification of ebselen and its analogues as potent covalent inhibitors of papain-like protease from SARS-CoV-2, Sci. Rep. 11 (2021) 3640, https://doi.org/10.1038/s41598-021-83229-6.

[45] J. Lu, et al., Ebsulfur is a benzisothiazolone cytocidal inhibitor targeting the trypanothione reductase of Trypanosoma brucei, J. Biol. Chem. 288 (2013) 27456–27468, https://doi.org/10.1074/jbc.M113.495101.

[46] R. Kitz, I.B. Wilson, Esters of methanesulfonic acid as irreversible inhibitors of acetylcholinesterase, J. Biol. Chem. 237 (1962) 3245–3249.

[47] C. Tapeinos, M. Battaglini, G. Ciofani, Advances in the design of solid lipid nanoparticles and nanostructured lipid carriers for targeting brain diseases, J. Control. Release 264 (2017) 306–332, https://doi.org/10.1016/j.jconrel.2017.08.033.

[48] P. Holzmuller, R. Bras-Goncalves, J.L. Lemesre, Phenotypical characteristics, biochemical pathways, molecular targets and putative role of nitric oxide-mediated programmed cell death in Leishmania, Parasitology 132 (Suppl) (2006) S19–S32, https://doi.org/10.1017/S0031182006000837.

[49] C.B. Ponte, et al., Miltefosine enhances phagocytosis but decreases nitric oxide production by peritoneal macrophages of C57BL/6 mice, Int. Immunopharmacol. 13 (2012) 114–119, https://doi.org/10.1016/j.intimp.2012.03.016.

[50] M.T. da Silva, I. Silva-Jardim, O.H. Thiemann, Biological implications of selenium and its role in trypanosomiasis treatment, Curr. Med. Chem. 21 (2014) 1772–1780, https://doi.org/10.2174/09298673206613119121108.

[51] E.H. Roma, et al., Impact of reactive oxygen species (ROS) on the control of parasite loads and inflammation in Leishmania amazonensis infection, Parasit. Vectors 9 (2016) 193, https://doi.org/10.1186/s13071-016-1472-y.

[52] N.C. Rochael, et al., Classical ROS-dependent and early/rapid ROS-independent release of Neutrophil Extracellular Traps triggered by Leishmania parasites, Sci. Rep. 5 (2015) 18302, https://doi.org/10.1038/srep18302.

[53] P.P. Carneiro, et al., The Role of Nitric Oxide and Reactive Oxygen Species in the Killing of Leishmania braziliensis by Monocytes from Patients with Cutaneous Leishmaniasis, PLoS One 11 (2016), https://doi.org/10.1371/journal.pone.0148084.

[54] M. Bodnar, P. Konieczka, J. Namiesnik, The properties, functions, and use of selenium compounds in living organisms, J. Environ. Sci. Health C Environ.

Carcinog. Ecotoxicol. Rev. 30 (2012) 225–252, https://doi.org/10.1080/10590501.2012.705164.
[55] S. Rashidi, et al., Selenium and protozoan parasitic infections: selenocompounds and selenoproteins potential, Parasitol. Res. 121 (2022) 49–62, https://doi.org/10.1007/s00436-021-07400-8.
[56] S.T. Stefanello, et al., Free radical scavenging in vitro and biological activity of diphenyl diselenide-loaded nanocapsules: DPDS-NCS antioxidant and toxicological effects, Int. J. Nanomed. 10 (2015) 5663–5670, https://doi.org/10.2147/ijn.S87190.
[57] M.A. Toro, et al., Probing the dimerization interface of Leishmania infantum trypanothione reductase with site-directed mutagenesis and short peptides, Chembiochem 14 (2013) 1212–1217, https://doi.org/10.1002/cbic.201200744.
[58] C.V. Ribeiro, et al., Leishmania infantum induces high phagocytic capacity and intracellular nitric oxide production by human proinflammatory monocyte, Mem. Inst. Oswaldo Cruz 115 (2020), https://doi.org/10.1590/0074-02760190408.